scientific reports

Check for updates

OPEN

Ethylenediaminetetraacetic acid conjugated with polyethylene glycol is a safe chelator for colonic epithelial denudation and intestinal epithelial replacement therapy

Yuka Matsumoto[1]✉, Yuta Murakami[2], Kazuto Suda[1], Mirei Takahasi[1], Kenichiro Nakai[2], Nozomi Ohta[2], Shihei Motofuji[2], Go Miyano[1], Hiroyuki Koga[1], Nobutaka Hattori[3], Kiichiro Tsuchiya[4], Atsuyuki Yamataka[1] & Tetsuya Nakamura[5]✉

Colonic epithelia can be replaced with small intestinal (SI) epithelia through de-epithelialization of the colon using ethylenediaminetetraacetic acid (EDTA), followed by SI organoid transplantation, to treat short bowel syndrome and intestinal failure. However, the low molecular weight (MW) of EDTA results in hypocalcemia, consequently hindering the clinical application of this bivalent cation chelator. Therefore, we aimed to synthesize a non-absorbable chelator for potential application in regenerative medicine. We conjugated polyethylene glycols (PEGs) of different MWs to EDTA to synthesize EDTA-PEGs with higher MWs. NMR and LC-TOF/MS analyses demonstrated the stability and chelating ability of EDTA-PEGs. Moreover, EDTA-PEGs mitigated hypocalcemia in mice. This effect was more pronounced in EDTA-PEGs with a higher MW than in EDTA. Furthermore, EDTA-PEGs de-epithelialized a targeted region of the mouse colon, replacing it with SI organoids to preserve SI features. This study provides a basis for the development of safe regenerative medicine utilizing EDTA-PEG.

Keywords Chelating agents, Intestinal organoids, Transplantation, Regenerative medicine

Short bowel syndrome (SBS) is a malabsorption disorder that involves a massive small intestine (SI) resection[1–3]. Patients with severe SBS supplement enteral nutrition with parenteral nutrition (PN). Furthermore, those with irreversible intestinal failure require intestinal transplantation to maintain health and growth. However, these treatment options may lead to severe liver failure secondary to long-term PN, or require lifelong immunosuppression following intestinal transplantation. Therefore, novel treatment strategies for SBS are required[4].

Organoids, which are self-organized three-dimensional multicellular structures that recapitulate the behavior of the original tissues[5], have attracted interest in regenerative medicine for intestinal diseases. Since SI epithelial organoids can be maintained and expanded ex vivo while retaining the original features essential for digestion and absorption[6,7], they are a potential cell source for cell therapy or tissue engineering in patients with SBS.

The epithelium of a colon segment in patients with SBS can be replaced by engrafting SI organoids onto the denuded colon[8,9]. Fukuda et al.[10] de-epithelialized the distal colon and engrafted SI organoids into the lumen in a heterotopic transplantation mouse model. The SI organoids regenerated the epithelium, whereas the SI phenotypes were heterotopically preserved[10]. Similarly, Sugimoto et al. developed a two-step surgical approach to assess the efficacy of small intestinalization of the colon (SIC) against SBS in rat models[11,12]. First, they dissected a segment of the proximal colon while preserving the vasculature, de-epithelialized its luminal surface,

[1]Department of Pediatric General and Urogenital Surgery, Juntendo University School of Medicin, 2-1-1 Hongo, Bunkyo-ku, Tokyo 113-8421, Japan. [2]Sanyo Chemical Industries, Ltd, 11-1, Ikkyo Nomoto-cho, Higashiyama-ku, 6050995 Kyoto, Kyoto-shi, Japan. [3]Department of Neurology, Juntendo University School of Medicine, 2-1-1 Hongo, Bunkyo-ku, Tokyo 113-8421, Japan. [4]Department of Gastroenterology, Institute of Medicine, University of Tsukuba, 1-1, Amakubo 2-chome, Tsukuba City 305-0005, Ibaraki Prefecture, Japan. [5]Department of Research and Development for Organoids, Juntendo University Graduate School, 2-1-1, Hongo, Bunkyo-ku, Tokyo 113-8421, Japan. ✉email: y.matsumoto.sg@juntendo.ac.jp; t.nakamura.sv@juntendo.ac.jp

transplanted SI organoids onto the denuded segment, and used the segment to create a stoma. After a week, they interposed the organoid-transplanted segment between the proximal end of the jejunum and ileocecal valve using end-to-end anastomosis, combining total jejunoileal resection and stoma closure[11]. SIC improved clinical symptoms and survival rate and resulted in body weight gain[11].

Physical interactions between the intestinal epithelium and the underlying basement membrane (BM) are mediated by integrins that function in a divalent cation-dependent manner[13–15]. Specifically, ethylenediaminetetraacetic acid (EDTA), a chelating agent that binds divalent metal ions such as calcium ion (Ca^{2+}) and Mg^{2+}, is used to loosen the binding between the colonic epithelium and the BM[10,11]. However, EDTA-based colonic de-epithelialization has adverse effects. EDTA salt forms[16] capable of depleting Ca^{2+}, such as disodium EDTA (EDTA-Na_2), are used for in vivo colonic de-epithelialization. However, they cause severe acute hypocalcemia when rapidly transferred into the bloodstream[17,18]. Therefore, the intravenous form of EDTA-Na_2 has been withdrawn from the market in most countries.

The risk of EDTA-related toxicity warrants the development of a strategy for preventing the absorption of chelating agents from the intestine or peritoneal cavity into systemic circulation during abdominal surgery. This could guarantee safe use of chelating agents in the SIC approach and facilitate their clinical application of SIC. As the size of a substance determines its absorption from the intestine and peritoneum[19–23], we hypothesized that EDTA coupled with macromolecules may become a non-absorbable chelating agent that can be used for colon de-epithelialization. Polyethylene glycol (PEG), a linear polymer composed of repeating oxyethylene units, is biocompatible and widely used in biomedical applications, including in bowel cleansing[24]. Moreover, the intestinal absorption of PEG decreases as its molecular weight (MW) increases[25,26]. Indeed, a previous study showed that PEGylation of a substance to increase its MW beyond 2000 reduced its absorption from the intestine and resulted in its retention in the intestinal tract[27]. Therefore, we theorized that the chelating function of the resultant compound, EDTA-PEG (E-PEG), could be locally confined to the intestinal lumen by choosing an appropriate compound from among E-PEGs of different sizes.

In this study, we synthesized new chemical compounds (E-PEGs) of different molecular sizes and assessed their chelator properties. We further examined their toxicity and in vivo applicability to provide a basis for the clinical application of regenerative medical therapies for patients with severe SBS.

Results

E-PEGs were successfully synthesized

E-PEGs were synthesized via esterification between EDTA and PEG. We used monomethoxy PEG (mPEG) as the polymer backbone because one of the two hydroxyl groups at both ends of this molecule is methoxylated. Thus, esterification would only occur on the unmethoxylated side, resulting in the addition of only one EDTA molecule per PEG polymer in the final product (Fig. 1a). Moreover, we used two anhydrous EDTA forms in which one or two pair(s) of the four carboxyl groups form cyclic carboxylic anhydride(s) to supply the EDTA backbone. These cyclic structures contributed to effective esterification with the mPEG hydroxyl groups through a ring-opening reaction (Fig. 1a).

We obtained two E-PEG types: an EDTA derivative with the mPEG polymer at one site and another with two mPEG polymers at two different sites (Fig. 1a). We first esterified mPEG polymers of different mean MWs (approximately 550, 2,000, or 4,000 Da). These were then reacted with EDTA possessing one cyclic carboxylic anhydride to obtain E-PEG1, E-PEG2, and E-PEG3 (Fig. 1a). We subsequently synthesized E-PEG4 through the esterification of mPEG with an approximate mean MW of 2,000 Da and anhydrous EDTA possessing two cyclic carboxylic anhydrides (Fig. 1a). Finally, we compared E-PEG4 with E-PEG3 to determine whether the properties of E-PEG are influenced by both its MW and number of ester bonds.

E-PEGs were successfully characterized

All products were characterized using ^{1}H-NMR spectroscopy (Supplementary Fig. S1, and Supplementary Table S1). ^{1}H-NMR peaks corresponding to the PEG methoxy group, PEG repeats, EDTA core, and ^{1}H adjacent to the esterification bond between PEG and EDTA were clearly observed in the spectra. The product with one PEG polymer at one EDTA site (one-PEG-conjugated) could be distinguished from that with two PEG polymers at two sites (two-PEG-conjugated). This was achieved because the ^{1}H in the one-PEG-conjugated EDTA backbone is chemically and magnetically non-equivalent, whereas that of the two-PEG-conjugated EDTA is equivalent. Supplementary Table S2 shows the percentage compositions of one- and two-PEG-conjugated EDTA, as well as unreacted mPEG and EDTA for each reaction product. The reactions with EDTA containing one and two cyclic carboxylic anhydrides predominantly yielded one- and two-PEG-conjugated EDTA, respectively (Fig. 1a). Furthermore, the reaction with EDTA containing one or two anhydrides led to the formation of low amounts of two- and one-PEG-conjugated EDTA as byproducts, respectively. The contents of the main products and byproducts of each reaction ranged from 94.3% to 97.8% (Supplementary Table S2).

To directly compare the carbon skeleton of raw materials (EDTA, mPEG550, mPEG2000 and mPEG4000) and E-PEGs (E-PEG1, E-PEG2, E-PEG3 and E-PEG4), we performed ^{13}C-NMR (Supplementary Fig. S2, and Supplementary Table S3). In addition to the peaks of the EDTA core, the PEG methoxy group, and the PEG repeats observed in the spectra of EDTA and mPEGs before coupling, we newly confirmed a carbon peak indicating the ester bond between PEG and EDTA in the spectra of E-PEGs after coupling. The results clearly demonstrated the successful coupling of EDTA and mPEGs.

An E-PEG1 solution was subjected to nine different conditions for 1 h and analyzed using ^{1}H-NMR to investigate the effects of temperature (25, 40, and 50 °C) and pH (4.0, 7.0, and 8.0) on the stability of E-PEGs. The ratio between the EDTA protons adjacent to the intramolecular ester bonds and those on the opposite sides (PEG sides) of the ester bonds was used to determine the stable E-PEG fraction under each condition. The ratios

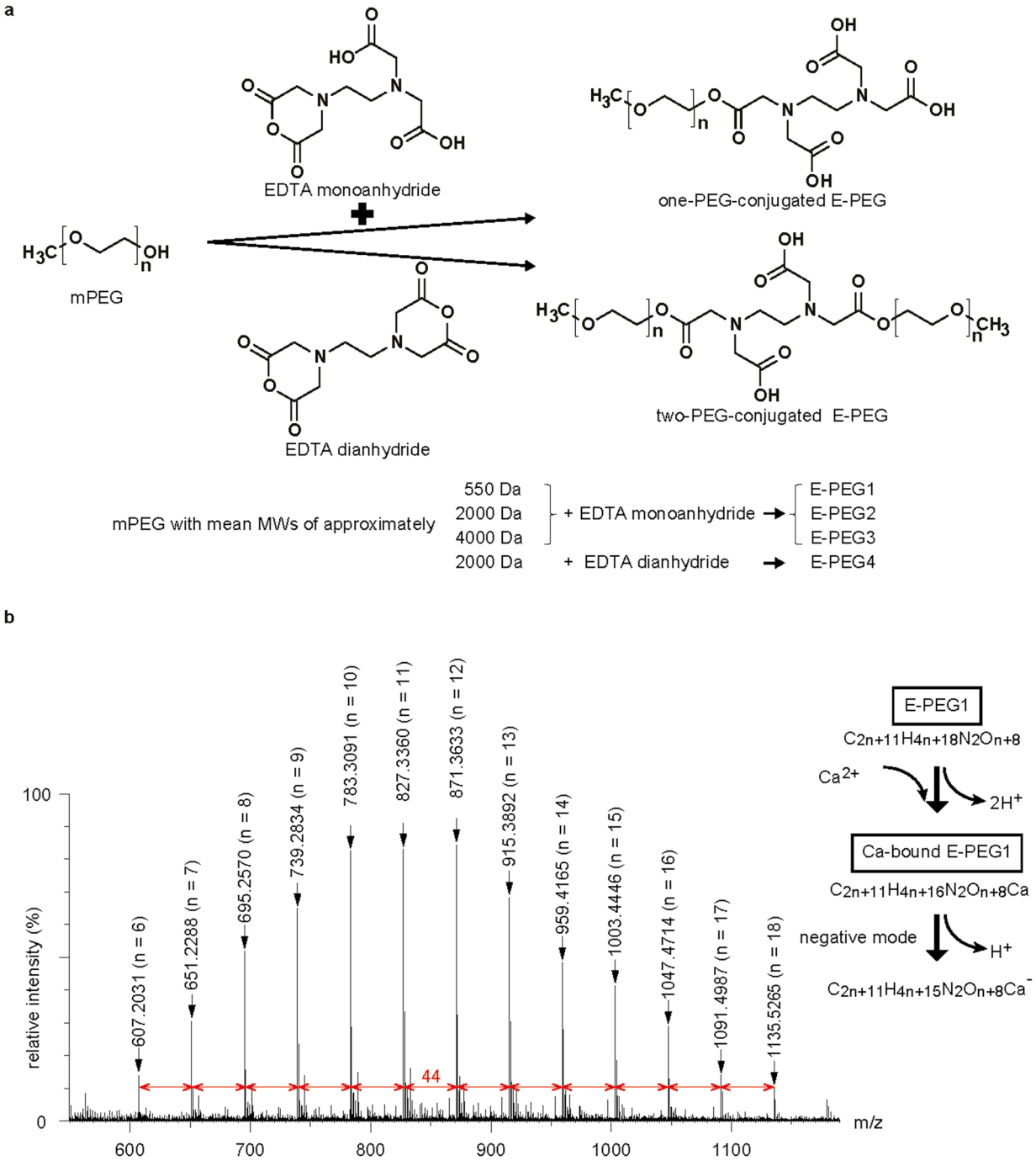

Fig. 1. Synthesis and characterization of E-PEGs. (**a**) Monomethoxy PEG (mPEG) has a methoxy group at one end. EDTA monoanhydride and EDTA dianhydride were reacted with mPEG to synthesize one- and two-PEG-conjugated E-PEGs, respectively. Reaction of EDTA monoanhydride with mPEG of mean MWs of approximately 550, 2,000, or 4,000 Da yielded E-PEG1, E-PEG2, or E-PEG3, respectively. Reaction of EDTA dianhydride with mPEG of mean MW of approximately 2,000 Da yielded E-PEG4. (**b**) UHPLC-QTof-MS^E analysis of the mixed solution of E-PEG1 and Ca. The scheme on the right shows the chemical formulas and transitions of protons during complex formation and MS analysis. The theoretical molecular weights of E-PEG1 with different number of oxyethylene repeats (n) are as follows: 827.3338 for $C_{33}H_{59}N_2O_{19}Ca$ ($n = 11$), and 783.3076 for $C_{31}H_{55}N_2O_{18}Ca$ ($n = 10$). The discrepancy between the theoretical and measured values was negligible.

obtained under all conditions were > 95%, indicating stability of the ester bonds between EDTA and mPEG (Table 1).

To assess the molecular weight distribution of E-PEGs and mPEGs, we performed gel permeation chromatography (GPC) (Supplementary Table S4). Although the obtained number-average molecular weight (Mn) and weight-average molecular weight (Mw) of E-PEGs were greater than those calculated by ^{1}H-NMR, we reasoned that this was because the calibration curve was constructed with PEGs. We found that polydispersity index (PDI = Mw/Mn) values of all E-PEGs were in the range of 1.02–1.12, confirming that they were uniformly monodispersed polymers.

We further assessed the cation-chelating ability of E-PEG1 by identifying the Ca-E-PEG1 complex in a mixed solution using TOF-MS (Fig. 1b). Several peaks that corresponded to an oxyethylene unit in the mPEG polymers were observed at 44 m/z intervals. These were consistent with molecular masses containing one Ca atom and one mPEG polymer possessing ethylene oxide repeats centered at approximately 10–12. These results demonstrate that E-PEG1 can form a complex with Ca^{2+} in a 1:1 ratio.

The Ca^{2+}-chelating ability of all E-PEGs was evaluated using Patton and Reeder's dye (PR dye) solution, an indicator of the chelatometric titration of Ca^{2+}. The titrant containing the Ca-PR complex turned purple when PR dye was first added. The color changed to blue when the solution was titrated against an E-PEG solution. This endpoint indicated that the Ca-PR complexes were completely replaced by equimolar Ca-E-PEG complexes[28]. This strongly suggests that all E-PEGs formed complexes with Ca^{2+} in a 1:1 ratio. (Supplementary Fig. S3).

To assess the complex bond stability, we calculated the binding constant (K) of EDTA or E-PEGs with Ca^{2+}. $K_{E-PEG1,}$ $K_{E-PEG2,}$ $K_{E-PEG3,}$ and K_{E-PEG4} were lower than K_{EDTA} (Supplementary Table S5). K_{E-PEG4} were lowest among K of all chelating agents, which may be attributed to the low number of carboxyl groups used for coordinate bond with Ca^{2+}; the number was three in one-PEG-conjugated E-PEGs (E-PEG1, E-PEG2, and E-PEG3), compared to two in two- PEG-conjugated E-PEG (E-PEG4).

E-PEGs effectively isolate colonic crypt in vitro

We investigated whether E-PEGs could dissociate the epithelial compartment from colonic tissues in vitro. Chemical treatment with EDTA-Na_2 and mechanical forces to intestinal tissues enable the isolation of intestinal epithelial structural units from non-epithelial components *in vitro*[5,13–15,29,30]. As expected, EDTA-Na_2 and E-PEGs released colonic crypts into the supernatant, whereas tissues in HBSS (Nacalai Tesque, Kyoto, Japan) yielded no crypts. The liberated crypt number was the highest in the tissues treated with EDTA-Na_2 at all concentrations. In addition, the crypt count decreased as the E-PEGs MW increased in tissues treated with E-PEGs (Fig. 2a). Treatment with 10 mM yielded the highest crypt counts for all the chelating agents (Fig. 2b). The 30 mM chelator resulted in a lower crypt count than the 10 mM treatment; this was partly attributed to the progressive dissociation of colonic crypts into single cells. We found no significant differences in crypt counts between the groups treated with 10 mM E-PEG3 and E-PEG4, suggesting that the de-epithelialization abilities of these two E-PEGs were similar regardless of the number of intramolecular esterification sites. These results show that the newly synthesized E-PEGs could free colonic crypts from colon tissues, although size-dependent attenuation of such effects might occur.

Intraperitoneal administration of E-PEG reveals acute toxicity to mice

We assessed the acute toxicity of intraperitoneally (i.p.) administered EDTA-Na_2 and E-PEGs in mice. The i.p. injection of EDTA-Na_2 at a lethal dose of 50 (LD50, 260 mg/kg) resulted in convulsions and eventual death within 20 min in two of the three examined mice. When E-PEGs were administered with EDTA-Na_2 at equimolar doses (0.70 mmol/kg), all mice survived beyond the observation period (one week) without symptoms (Fig. 3a). When the E-PEG dose was doubled (1.40 mmol/kg), two of the three mice injected with E-PEG1 died, whereas all mice in the E-PEG2 group survived; only one mouse exhibited short-term carpopedal spasms immediately after injection. E-PEG3 and E-PEG4 mice showed no signs of hypocalcemia, suggesting that increasing the molecular mass of E-PEGs can reduce acute toxicity. It has been reported that, in cultured cells, low molecular weight PEG could enter the cytoplasm by passive transport and cause cytotoxicity due to the molecular crowding effect[31]. Although administration of E-PEG1 and E-PEG2 caused physical findings of hypocalcemia, it is also suggested that the crowding effect on cells throughout the body might be the cause of death. Thus, to confirm the direct involvement of hypocalcemia, we measured the serum Ca levels in mice 2 min after the i.p. injection of 1.40 mmol/kg EDTA-Na_2 and E-PEGs to directly attribute the acute toxicity symptoms to hypocalcemia. The serum Ca level in mice treated with EDTA-Na_2 (4.60 ± 0.57 mg/dL) was markedly lower than that in E-PEG-treated mice (Fig. 3b). Moreover, the degree of hypocalcemia in E-PEG-injected mice was mitigated as the E-PEG molecular size increased. The serum Ca levels in the E-PEG3 and E-PEG4 groups were comparable to those in the control group. This indicates that the acute toxicity of EDTA-Na_2 is directly linked to a rapid drop in the serum Ca levels, and that this hypocalcemic effect could be prevented by coupling EDTA with PEG polymers.

Temperature (°C)	pH 4	pH 7	pH 8
25	97.2	99.1	95.6
40	104.2	101.9	96.0
50	102.6	102.0	99.0

Table 1. The binding rate of the ester bond between mPEG and EDTA anhydride.

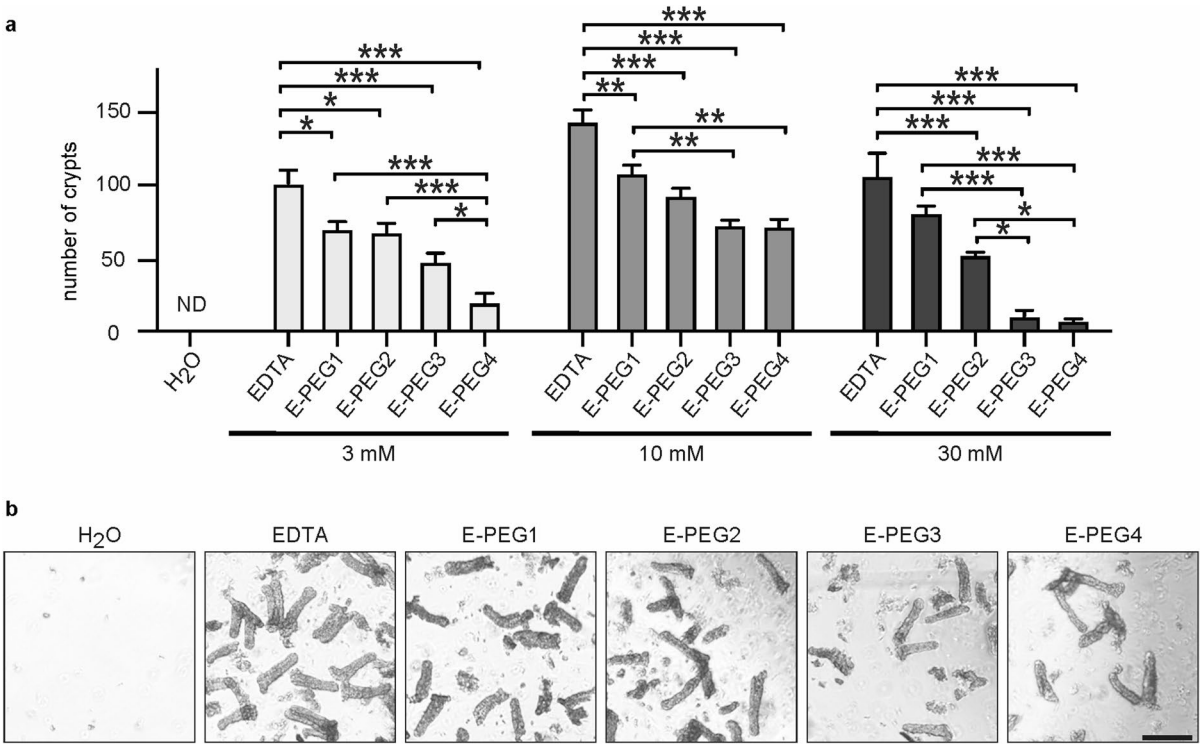

Fig. 2. The efficiency of E-PEGs in colonic crypt isolation in vitro. (**a**) The number of crypts isolated using different concentrations of EDTA and E-PEGs. Data for 50 µL drops of crypt suspension are presented ($n = 6$). ND: not detected. Data are expressed as the mean ± SEM (*$P < 0.05$, ** $P < 0.01$, *** $P < 0.001$). (**b**) Representative images of the isolated crypts (scale bar, 200 µm).

The clinical manifestations and the serum Ca levels of the E-PEG3 and E-PEG4 groups did not differ; therefore, we excluded E-PEG3 from subsequent analyses.

Assessment of the toxicity and de-epithelialization efficiency of E-PEGs in an intracolonic administration model

We assessed the systemic toxicity and effects on the mucosa when the colonic lumen was perfused with EDTA-Na_2 or E-PEGs using three models (Supplementary Fig. S4). The mice were euthanized and subjected to serum Ca analysis after perfusion with EDTA-Na_2 (10 mM) (Supplementary Fig. S4). A longer perfusion length of the colon corresponded with a lower serum Ca level, reaching 5.2 mg/dl when the whole colon (8 cm) was perfused.

Among the three models, we applied the whole-colon (8 cm) perfusion model for comparative assessment of the toxicity of EDTA-Na_2 (10 mM), E-PEGs (10 mM), and the control (water) (Fig. 4a). The serum Ca level of the EDTA-Na_2 perfusion group was significantly lower than that of the control group. However, the decrease in serum Ca among the E-PEG groups was mitigated as the MW of the perfused E-PEGs increased. Additionally, the serum Ca level in the E-PEG4 group remained comparable to that of the control (Fig. 4b).

Light microscopy of the colon from the euthanized mice revealed irregularly shaped areas exhibiting higher light permeability than the regions close to the catheter insertion site in the proximal colon. These features were observed in the colons of mice perfused with EDTA-Na_2 or E-PEGs, but not in those of the controls (Fig. 4c). We hypothesized that these light-transmissive areas had thinner colonic walls that preserved the underlying non-epithelial tissues, but lacked the epithelium, allowing for the quantitative assessment of de-epithelialized colonic areas. As expected, the degree of de-epithelialization along the colon was not uniform. We histologically classified the degree of epithelial denudation into three levels: level 1, no denudation; level 2, intermediate denudation; and level 3, complete denudation (Supplementary Fig. S5). The percentage of level 3 areas correlated well with that of the light-transmissive area (Fig. 4d, Supplementary Fig. S5). Therefore, the light-transmissive area was valid for use in the quantitative evaluation of de-epithelialized areas. These results demonstrate that the de-epithelialization ability was higher for EDTA-Na_2 than for the other chelators, and this declined as the E-PEG molecular size increased when the chelators were administered in the same amount and at the same flow rate (Fig. 4d).

We further investigated whether the de-epithelialization area induced by E-PEG4 could be expanded by extending the perfusion time. When the whole colon was perfused with E-PEG4 for 50 min, the denuded area increased to a level comparable to that induced by 30-min treatment with EDTA-Na_2 (Fig. 4e, left). The serum Ca level after 50 min of perfusion with E-PEG4 was similar to that in the control group (Fig. 4e, middle). This demonstrates that, although the relative chelating potential of larger E-PEGs is lower than that of EDTA-Na_2,

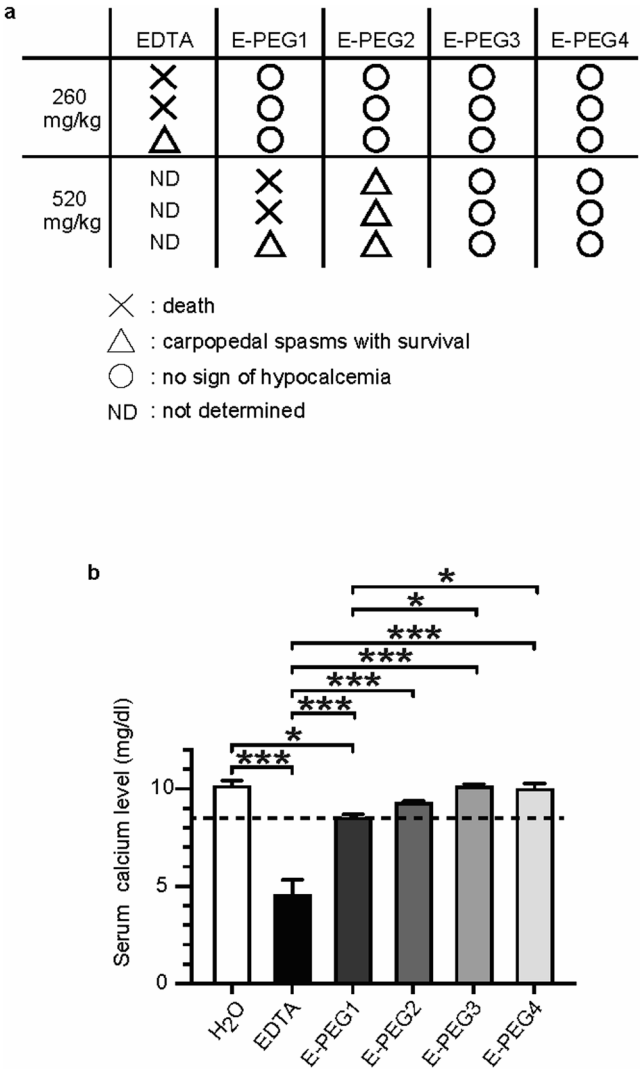

Fig. 3. Acute toxicity resulting from the intraperitoneal (i.p.) administration of EDTA and E-PEGs. (**a**) Clinical manifestations of severe hypocalcemia that emerged one week after the i.p. administration of 1×LD50 and 2×LD50 of EDTA-Na_2 or equimolar doses of E-PEGs. (**b**) Serum Ca levels 2 min after the i.p. administration of H_2O, 2×LD50 of EDTA-Na_2, or equimolar doses of E-PEGs ($n = 6$). A dashed line indicates the lower limit of the serum Ca levels. Data are expressed as the mean ± SEM (*$P < 0.05$, *** $P < 0.001$).

improvement in the local chelator application methods may increase their de-epithelialization competence without increasing their systemic toxicity.

To determine whether the low systemic toxicity of E-PEG4 compared to that of EDTA-Na_2 was due to its low influx from the colon into the systemic circulation, we analyzed the serum concentrations of these two compounds after perfusion for 50 min in the whole-colon perfusion model using LC-MS/MS. The serum concentration of EDTA-Na_2 was 2.02 mM, whereas that of E-PEG4 was only 0.03 mM (Fig. 4e right, Supplementary Fig. S6). This demonstrated that E-PEG4 was less toxic than EDTA-Na_2 because there was less absorption of E-PEG4 in the colon.

The colon can be segmentally de-epithelialized through targeted E-PEGs perfusion

We investigated whether E-PEGs could be used for the targeted de-epithelialization of a certain colon length. The construction of the mouse model is shown in Fig. 5a. The target site was clamped on both the proximal and distal sides to prevent leakage of the luminal chelators (Fig. 5b). Moreover, the mesenteric vasculature was clamped during 10 mM chelator perfusion (5 min) to enhance EDTA-Na_2-mediated local de-epithelialization[11]. The denuded area was light-transmissive (Fig. 5c). Furthermore, the EDTA-Na_2-treated colonic segments showed approximately 40% de-epithelialization, and this proportion decreased as the E-PEG molecular size increased (Fig. 5d).

We further investigated whether the de-epithelialization area induced by E-PEG4 could be expanded by extending the perfusion time (from 5 min to 7.5 min). The denuded area increased from approximately 20% to 30%, indicating that de-epithelialization efficiency could be controlled by refining the local application of

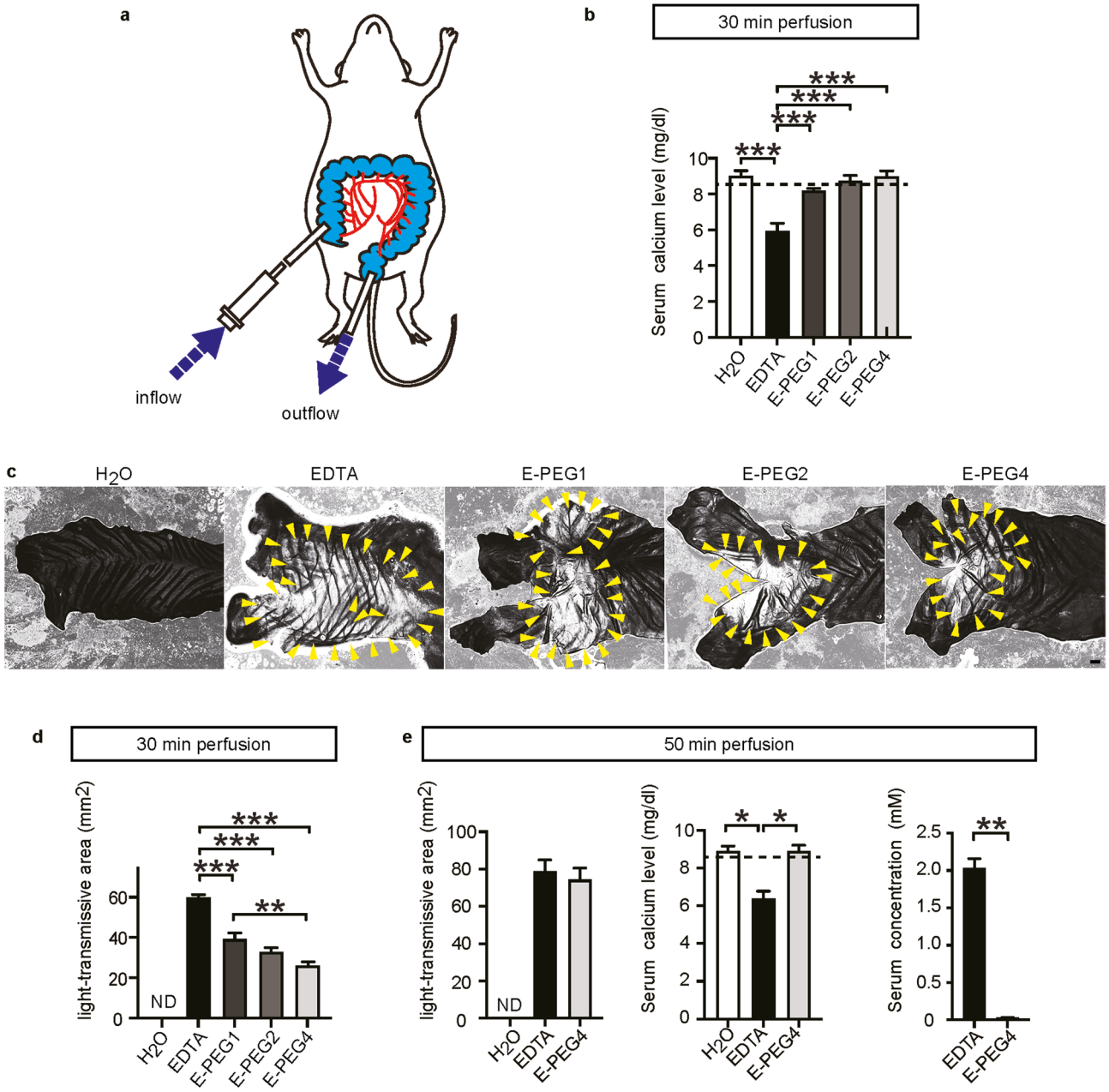

Fig. 4. Toxicity and de-epithelialization efficiency of EDTA and E-PEGs in a whole-colon perfusion model. (**a**) Schematic representation of the mouse laparotomy model for whole-colon perfusion. (**b**) The serum Ca levels immediately after 30 min of perfusion with H_2O or 10 mM of the chelating agents through the whole colon ($n = 5$). (**c**) Representative images of the proximal colon after perfusion (scale bars, 1 mm). Arrowheads indicate the light-transmissive areas under microscopic observation. (**d**) Measurement of the light-transmissive areas of the colon after 30 min of perfusion ($n = 5$). (**e**) Measurements of the light-transmissive areas (left) ($n = 5$), serum Ca levels (middle) ($n = 5$), and serum concentration of EDTA, and E-PEG4 after 50 min of perfusion (right) ($n = 6$). See also Supplementary Fig. S6. Dashed lines indicate the lower limit of the serum Ca levels. ND: not detected. All data are expressed as the mean ± SEM. (*$P < 0.05$, ** $P < 0.01$, *** $P < 0.001$).

E-PEGs to the target colon (Fig. 5e). Thus, we confirmed that the colon could be segmentally de-epithelialized via the targeted perfusion of E-PEGs using a transluminal approach.

E-PEG4-induced colon de-epithelialization facilitates engraftment of transplanted SI organoids

We investigated whether E-PEGs could generate a denuded colon that allows the engraftment of transplanted SI epithelial organoids[10,11]. Targeted de-epithelialization of the proximal colon (approximately 1-cm long) via 5-min perfusion of EDTA-Na_2 (10 mM) or E-PEG4 (10 mM) with concomitant vascular clamps did not cause lethality

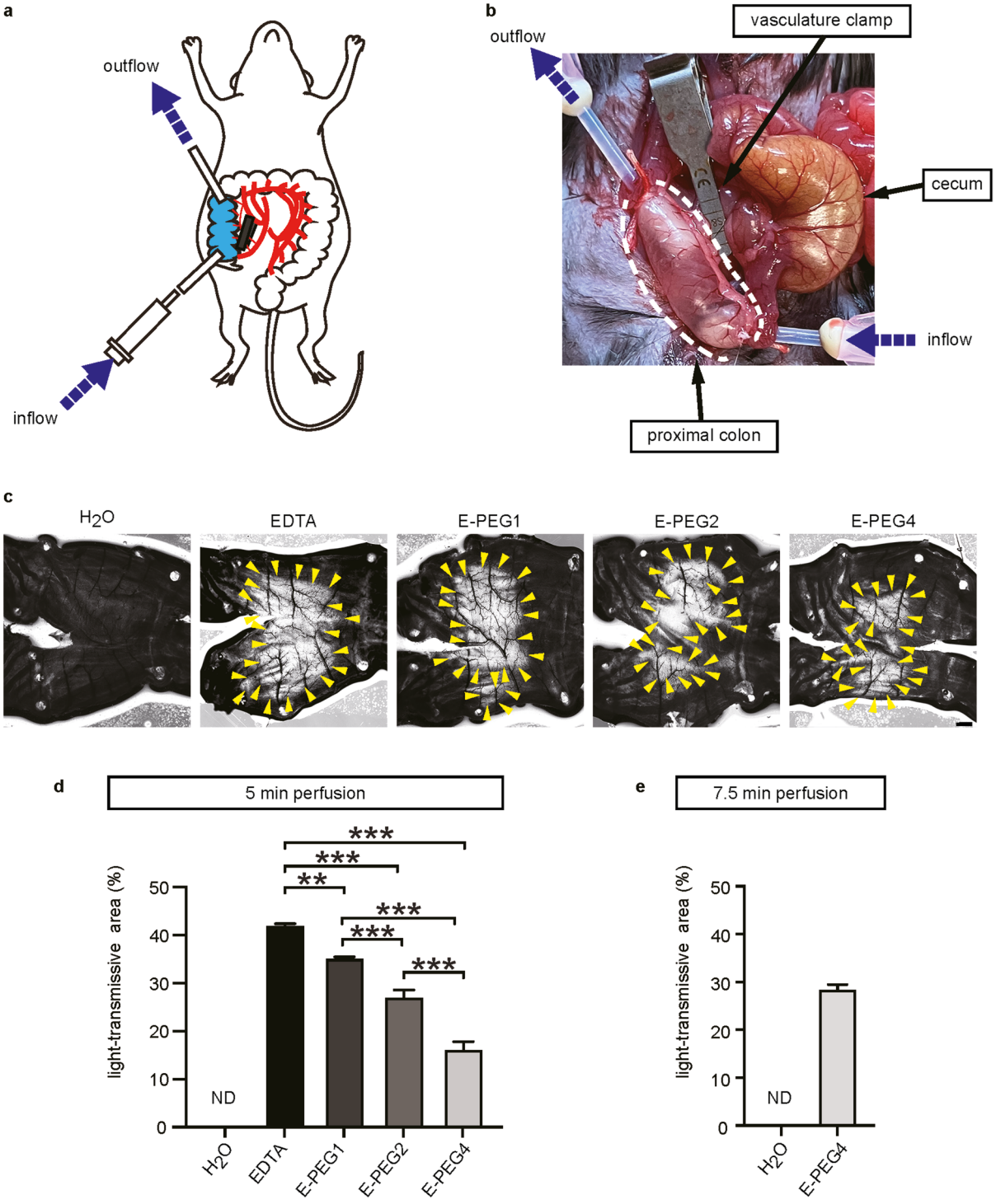

Fig. 5. De-epithelialization efficiency of EDTA and E-PEGs in a proximal colon perfusion model. (**a**) Schematic representation of the laparotomy mouse model for proximal colon perfusion. (**b**) An image demonstrating the proximal colon perfusion procedure. (**c**) Representative images of the targeted colon after perfusion (scale bars, 1 mm). Arrowheads indicate the light-transmissive areas. (**d**) Measurement of the light-transmissive areas after 10 mM EDTA, 10 mM E-PEGs, and water (control) perfusion for 5 min ($n = 5$). (** $P < 0.01$, *** $P < 0.001$). (**e**) Measurement of the light-transmissive areas after 10 mM E-PEG4 and water (control) perfusion for 7.5 min ($n = 5$). Data are expressed as the mean ± SEM. ND: not detected.

in mice. Additionally, it led to survival longer than 1 month (Supplementary Fig. S7). Histological analysis one month after de-epithelialization revealed that no infiltration of inflammatory cells was observed in the colons treated with EDTA-Na_2 or E-PEG, as in the control colon where treatment with chelators was not performed. Moreover, no obvious histological changes such as fibrosis or resulting stenosis were observed in the colon of all groups. Transplantation experiments were performed using SI organoids derived from EGFP-transgenic mice. The SI organoid suspension was subsequently infused into the lumen. Well-demarcated $EGFP^+$ areas were observed in the colons of EDTA-Na_2- or E-PEG4-treated mice euthanized four weeks post-transplantation (Fig. 6a, Supplementary Fig. S8). Moreover, some parts of the $EGFP^+$ layer changed into invaginated structures reminiscent of intestinal crypts (Fig. 6b, Supplementary Fig. S8).

Structures protruding toward the lumen of the $EGFP^+$ epithelia were observed in the both EDTA-Na_2- and E-PEG4-treated mouse colons; these resembled the villus structure in the SI. $EGFP^+$ epithelia contained the SI-specific functional epithelial cells $OLFM4^+$ (SI stem cells), sucrase-isomaltase $(SIase)^+$ (absorptive cells), and LYZ^+ cells (Paneth cells) (Fig. 6c, Supplementary Fig. S8). We also found cells positive for SLC10A2, a bile acid transporter expressed in the SI, in the $EGFP^+$ epithelium. The $EGFP^+$ epithelia further contained cells that were positive for Ki67, MUC2, CHGA, which are marker proteins of proliferative, goblet, and enteroendocrine cells, respectively. These are common cell types in both the SI and colon. In contrast, CA2, a marker protein of the colonic epithelium, was not expressed in the $EGFP^+$ epithelia. Moreover, the numbers of LYZ^+, $CHGA^+$, and $MUC2^+$ cells per villus-crypt unit in the $EFGP^+$ epithelium of EDTA-Na_2 and E-PEG-treated mice were comparable to those in the ileum of non-operated mice (control) (Fig. 6d). These results demonstrate that the E-PEG4-induced de-epithelialization of the colon enables transplanted SI organoids to engraft and mature into SI-type epithelia in denuded tissues.

Discussion

We synthesized E-PEGs and characterized their toxicity to develop new chelating agents for colonic de-epithelialization in vivo. E-PEGs were less toxic than EDTA. In addition, they loosened the binding interactions between the epithelial and non-epithelial compartments in the colon. Finally, the colonic segment denuded by E-PEG4 treatment enabled successful engraftment of SI epithelial organoids, which retained the SI phenotypes even in a heterotopic environment after transplantation.

Consistent with previous findings[17,18], EDTA-Na_2 i.p. injection led to fatal convulsions. Furthermore, i.p. and intracolonic administration significantly reduced the serum Ca levels in mice. The low toxicity of E-PEGs was inversely correlated with the molecular size of E-PEG. As the E-PEGs de-epithelialization efficiency decreased with an increase in molecular size (Figs. 2a and 4d, and Fig. 5d), the low toxicity of larger E-PEGs may be explained by their low chelating ability. We considered two possible reasons for this: (1) the presence of steric hindrance, which renders it difficult for the anionic sites to come close to Ca^{2+} in E-PEGs; and (2) the decrease in molecular collisions of E-PEGs with Ca^{2+} owing to the higher viscosity of the E-PEG solution than that of EDTA. However, the low systemic toxicity of E-PEGs may also reflect a low E-PEGs influx from the local colon tissue into the systemic circulation. Urinary EDTA excretion accounts for approximately 80% and 10% of the intraperitoneal and orally administered doses, respectively[32]. Therefore, a substantial amount or a certain proportion of EDTA in the peritoneal space or within the gastrointestinal tract, respectively, is absorbed into the bloodstream. The molecular size of a substance determines the efficacy of its peritoneal absorption[33]. This also applies to the transfer of substances across gut tissues[21–23]. The permeability of the gastrointestinal mucosa to PEG is MW-dependent[25,26]; thus, PEGs with higher MWs can be used as nonabsorbable lavage solutions[24]. To our knowledge, the present study is the first to measure serum concentrations of EDTA and E-PEG4 after whole-colon perfusion (Fig. 4e right). Although we showed that E-PEG4 was less absorbable than EDTA in the colon, comprehensive investigation of the pharmacokinetics and pharmacodynamics including systemic distribution and clearance of all E-PEGs after local administration is required for the development of chelating agents that enable safe and efficient intestinal de-epithelialization.

The toxicity of E-PEG4 was the lowest, whereas its molecular size was higher than those of EDTA, E-PEG1, and E-PEG2. In addition, the de-epithelialized areas were the lowest in E-PEG4-treated tissues. However, a low de-epithelialization efficiency does not necessarily indicate a limitation in maximizing the de-epithelialized areas. No decrease in the serum Ca levels was detected, even when the perfusion time with E-PEG4 was extended from 30 to 50 min (Fig. 4e). This indicates that E-PEG4 is hardly absorbed through the colonic tissue, even during progressive de-epithelialization changes that may enhance the permeability of the colon. Brady et al.[34]. reported that the urinary excretion of PEG4000 administered via oral intestinal lavage to patients with inflammatory bowel disease is comparable to that of normal controls, indicating that PEGs of this molecular size do not readily enter the bloodstream from the damaged intestine. Therefore, we hypothesize that E-PEG4 is as non-absorbable as PEG4000, even through progressively denuded mucosa. Thus, it may be a useful chelator for colonic de-epithelialization if its application can be optimized to the target colonic mucosa.

In this study, we modified the surgical techniques for colonic de-epithelialization using our own model[10,35]. First, we clamped the vascular pedicle to nourish the target colon during a short chelator treatment period. Temporary interruption of blood flow to the target colon using a vascular clamp ameliorated the efficiency of EDTA de-epithelialization in a rat model[11]. Hence, we used this technique. Interrupting the vascular supply to the targeted proximal colon for 5 min enhanced the de-epithelialization efficiency of EDTA and E-PEG4. Another modification was the removal of the epithelium after treatment with chelators. The brushing device utilized in previous studies[10,35] was difficult to apply for the de-epithelialization of the mouse proximal colon, which is substantially thin and easy to move around during the procedure because it is not fixed in the abdominal cavity. Instead, hydrodynamic pressure is used to physically remove the epithelium after chelator treatment. Flushing the lumen of the target colon with Ca- and Mg-free fluids effectively washed out the detached epithelia. The technical modifications in this study demonstrate the feasibility of segmental de-epithelialization of the

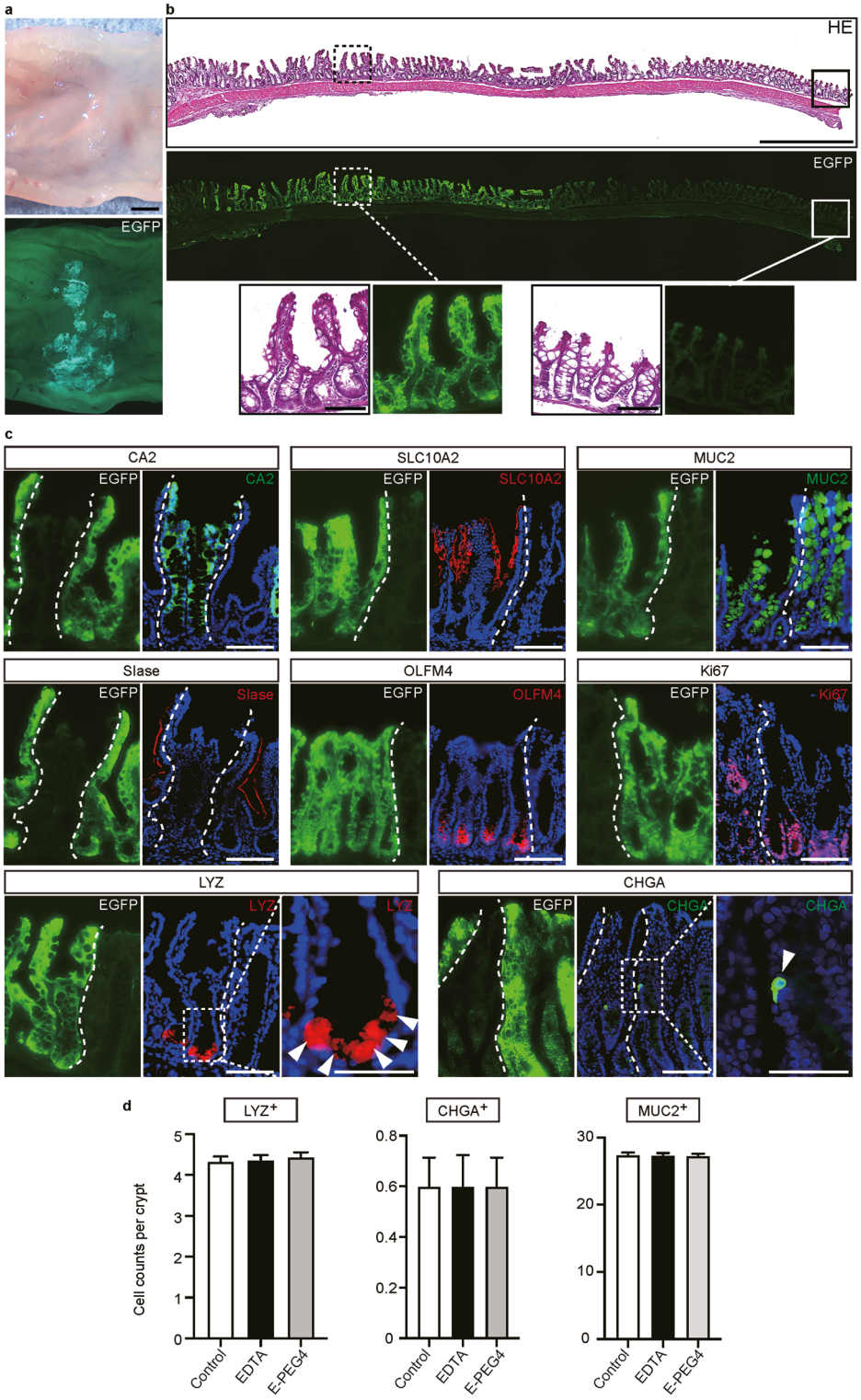

site that preserves colonic continuity. However, these techniques are not readily applicable in clinical practice. Interrupting and reopening blood vessels in the target colon is impractical because it induces intestinal ischemia-reperfusion injury[36,37]. Moreover, de-epithelialization surgery on a colon with a large diameter, such as the human colon, can be safely and reliably performed using devices such as soft brushes instead of luminal flushing. To facilitate the clinical applicability of this de-epithelialization strategy, future studies should enhance the effect of chelators on the target colonic mucosa without clamping its vessels during surgery. Furthermore, future studies are required to enable the application of mechanical forces to accelerate the detachment of the epithelium, especially for larger animals including humans.

There remain many limitations and future challenges in this study. As this study only evaluated the acute toxicity of E-PEGs, future studies will be important to evaluate long-term toxicity. It is also important to confirm the long-term viability and functionality of the recipient in E-PEG-treated proximal colon SIC model. In

◀**Fig. 6**. Analyses of the SI-derived graft transplanted onto the de-epithelialized colon denuded with E-PEG4. (**a**) The proximal colon of the recipient mouse four weeks after transplantation. The top shows the stereoscopic image and the bottom is its EGFP fluorescence image (scale bar, 1 mm). (**b**) H&E staining (top) and its EGFP fluorescence image (middle) of the recipient mouse colon are shown. High-power views of an $EGFP^+$ region in dashed boxes and an $EGFP^-$ region in lined boxes are shown on the bottom, respectively. (scale bars, 1 mm in low-power views and 100 μm in high-power views). (**c**) EGFP fluorescence of the sections analyzed are shown on the left of each panel. Their neighboring sections were subjected to immunofluorescence staining for CA2, SLC10A2, MUC2, SIase, OLFM4, Ki67, LYZ, and CHGA with DAPI staining (scale bars, 100 μm). High-power views of the area in the dashed boxes are also shown on the right for the LYZ and CHGA data (scale bars, 50 μm). Arrowheads point to LYZ^+ or $CHGA^+$ cells. Dashed lines indicate borders between $EGFP^+$ and $EGFP^-$ epithelia. (d) Quantification of the components of secretory cells. Mean cell counts of LYZ^+ or CHGA, or $MUC2^+$ cells per crypt–villus unit are presented for the ileum of non-operated mice (control), and for the $EFGP^+$ graft of EDTA- and E-PEG4-treated mice ($n = 15$).

addition, detailed biodistribution studies using E-PEGs which are labeled by isotopes are also pivotal. Potential immunogenicity of E-PEGs is also an important issue. Since it has been reported that anti-PEG antibody may appear against PEGylated products[38], the countermeasure to address this might be required. To apply SIC in human clinical practice, it is necessary to organize a system for manufacturing clinical-grade E-PEGs in quantities suitable for human use. Furthermore, since humans and mice differ in many features, from the effects of chelating agents on the epithelium[5,29] to the body size, it is necessary to optimize the conditions of E-PEGs administration and to develop and use a device fitted to SIC in large animals.

Although organoid-based regenerative medicines for SBS treatment have gained substantial research interest, complete ex vivo small intestine regeneration from organoids remains difficult. Replacing part of the epithelium of the remnant colon in patients with SBS with an SI epithelium does not require the construction of de novo vasculature of graft tissues. This technique may also help regenerate the digestive and absorptive functions of SI over a large colon area. Transplantation of organoids derived from the SI epithelium of a patient may eliminate the need for immunosuppressive treatment during SI transplantation therapy. In this study, the synthesized chelating agents were safely and effectively used to de-epithelialize the colon in vivo. Further experiments that may facilitate the implementation of translational research using E-PEG are required to enable the development of regenerative medicines to treat SBS and intestinal failure.

Materials availability

There are restrictions to the availability of E-PEGs because of a pending patent.

Materials and methods

Mice

All animal procedures were performed in accordance with the Basic Animal Care and Experimental Guidelines of the Ministry of Health, Labour and Welfare of Japan and the ARRIVE 2.0 guidelines. All animal experiments were approved by the Institutional Animal Care and Use Committee of the Juntendo University (Protocol 2023235). We used 7- to 8-week-old male C57BL/6J mice (CLEA Japan, Inc., Tokyo, Japan). Cells for transplantation experiments were obtained from male EGFP-transgenic mice with a C57BL/6 background (The Jackson Laboratory Japan, INC., Kanagawa, Japan)[39].

Materials

E-PEGs were synthesized by reacting EDTA anhydride with mPEG. Next, mPEG with a mean MW of approximately 550 Da (mPEG550) (NOF CORPORATION, Tokyo, Japan) was used to synthesize E-PEG1. mPEG2000 and mPEG4000 with mean MWs of approximately 2,000 and 4,000, respectively, were synthesized by polymerizing ethylene oxide (Senbokusanso Inc., Osaka, Japan) to mPEG550. Finally, EDTA monoanhydride was synthesized from EDTA dianhydride (Tokyo Chemical Industry Co. Ltd. (TCI), Tokyo, Japan) as described below.

Synthesis of EDTA monoanhydride

EDTA dianhydride (100 g) was dissolved at 90 °C using N, N-dimethylformamide (DMF) (FUJIFILM Wako Pure Chemical Corporation, Tokyo, Japan) (472.1 g). After cooling down to 75 °C, the DMF (94.3 g) and H_2O (7 g) mixture was added dropwise over 2 h. It was then stored for another 2 h at 75 °C, and EDTA monoanhydride was subsequently separated through filtration under reduced pressure. This resulted in 62% yield at 93% purity.

Synthesis of one-PEG-conjugated EDTA (E-PEG1, E-PEG2, and E-PEG3)

The mPEGs were dissolved in DMF. N, N-Diisopropylethylamine (DIPEA) (TCI) and EDTA monoanhydride were added to the mPEGs/DMF solution at 60 °C. Next, mPEG550, mPEG2000, and mPEG4000 were reacted with EDTA monohydride for 5, 5, and 12 h, respectively. T-butyl methyl ether (MTBE) (Nacalai Tesque) was then added to obtain E-PEG1, E-PEG2, and E-PEG3 via vacuum filtration and desiccation. The weight of the materials that reacted with 100 g of mPEG550, mPEG2000, and mPEG4000 were as follows: DMF: 486.4, 470.2, and 343.3 g; DIPEA: 22.7, 2.1, and 4.3 g; EDTA monoanhydride: 50, 14.9, and 10.5 g; MTBE: 3,886.4, 3,668.1, and 2,637.8 g. The yield and purity were described in Supplementary Table S2.

Synthesis of two-PEG-conjugated EDTA (E-PEG4)

mPEG2000 (100 g) was dissolved in DMF (466.7 g), followed by the addition of DIPEA (7.4 g) and EDTA dianhydride (7.4 g) at 25 °C and reaction for 5 h. The mixture was filtered under vacuum to obtain E-PEG4 after the addition of MTBE (3,122.2 g). The yield and purity were described in Supplementary Table S2.

^{1}H-NMR spectroscopy

^{1}H-NMR spectroscopy was performed using an AVANCEIII HD40 (Bruker Japan Co., Ltd., Kanagawa, Japan). ^{1}H-NMR spectroscopy was performed at 400 MHz using D_2O as the solvent for the structural characterization of the E-PEGs (Supplementary Table S1).

The average MW of the E-PEGs was calculated from the molar ratios of the main and accessory components (Supplementary Table S2). Their purity was represented as the percentage weight of E-PEGs relative to all synthetic compounds, including impurities of unreacted mPEG and EDTA. The stability of the ester bond between mPEG and EDTA anhydride was calculated as the residual binding ratio (RR) (%) of the methylene group adjacent to the ester bond to the methoxy group at one end of the E-PEG under different conditions (Table 1).

RR was calculated as shown in equation. (1):

$$\mathrm{RR}\ (\%)\ =\ 100\ \times\ \frac{a_{post}}{a_{pre}} \tag{1}$$

where a_{pre} and a_{post} are the binding rates of the methylene group to the methoxy group before and after subjecting E-PEGs to different conditions and can be expressed as shown in equation. (2):

$$Binding\ \mathrm{rate}\ (\mathrm{a})\ (\%)\ =\ 100\ \times\ \frac{\frac{g_1}{2}}{\frac{g_2}{3}} \tag{2}$$

where g_1 is the integrated value of the signal derived from the methylene group adjacent to the oxygen atom of the ester bond and g_2 is the signal derived from the methoxy group.

^{13}C-NMR spectroscopy

^{13}C-NMR spectroscopy was performed using an AVANCEIII 400 (Bruker Japan Co., Ltd., Kanagawa, Japan). ^{13}C-NMR spectroscopy was performed at 100 MHz using DMSO-d_6 as the solvent for the structural characterization of the E-PEGs (Supplementary Table S3).

Gel permeation chromatography

Number-average molecular weight (Mn), weight-average molecular weight (Mw) and polydispersity index (PDI = Mw/Mn) of E-PEGs and mPEGs were determined by gel permeation chromatography (GPC) (Supplementary Table S4). GPC was performed using Prominence chromatograph (Shimazu, Kyoto, Japan), Shodex OHpak SB-G + SB-803 HQ + SB-804 HQ columns (Resonac Corp.,Tokyo Japan) connected in series with a RID-10 A (Shimazu) detector. Four mg of samples were dissolved in 2 ml of an eluent, 0.1 M sodium nitrate solution containing 10% acetonitrile, and filtered through a 0.45 µm. The solution were analyzed using a chromatographic system with an eluent flow rate of 0.5 ml/min, an injection volume of 100 µl at 40 °C.

UHPLC-Qtof-MS^{E} analyses

The conditions for the UHPLC-Qtof-MS^{E} analysis using an ACQUITY H-Class UPLC system (Nihon Waters K.K., Tokyo, Japan) connected to a Xevo G2-XS Qtof mass spectrometer (Nihon Waters K.K.) are listed in Supplementary Table S6. High-accuracy MS was performed using MassLynx 4.2 (Nihon Waters K.K.). The MS^{E} data were acquired in continuum mode using the ramp collision energy and two scan functions: low collision energy, 10 V; and high collision energy ramp, 30 V. All analyses were carried out using an independent reference spray via Lock Spray interference.

Ca^{2+} complexometric titrations using PR dye

The ability of EDTA to form complexes with Ca^{2+} was assessed via chelate titration using PR dye (Dojindo Laboratories, Tokyo, Japan) according to the manufacturer's instructions. The molar ratio of the chelating agents to Ca^{2+} was calculated based on the amount of added chelating agent. Titration was performed five times for each chelating agent, and the mean value was determined (Supplementary Fig. S3).

Binding constant of Ca^{2+} with EDTA and E-PEGs

Ca^{2+} forms a complex with the chelating agents according to the following reaction equation: $\mathrm{Ca2+}\ +\ A\ \rightleftharpoons\ \mathrm{Ca}-A$

$$\mathrm{K}\ =\ \frac{[\mathrm{Ca}-\mathrm{A}]}{[\mathrm{Ca2+}]\,[\mathrm{A}]}$$

In the equation, A is the chelating agent, and K is the complex formation constant. Arsenazo III, which changes color when bound to Ca^{2+}, and the chelating agents were mixed in different ratios and added to a Ca^{2+} (2.4 mM) solution. The absorbance of each mixed solution differed due to the difference in the complex formation constant between the chelating agent and Arsenazo III. Since the complex formation constant of Arsenazo III

was already known, the relative complex formation constant of each E-PEG to Arsenazo III was calculated from the absorbance of the mixed solution[40].

In vitro assay of colonic crypt isolation efficiency

The distal half of the colonic tissue was minced into small pieces using a razor. Each sample was suspended in HBSS, transferred into 1.5 mL tubes, and shaken using a microtube mixer for 10 min at room temperature for washing. This procedure was repeated twice. After centrifugation, the samples were suspended in 1 mL of chelating agent at different concentrations at 37 °C and stored for 30 min. The samples were then centrifuged and resuspended in HBSS before 4% paraformaldehyde (0.5 mL) (Nacalai Tesque) was added. The number of crypts in 50 μL droplets was counted using an optical microscope. ($n = 6$)

Intraperitoneal and intracolonic administration of the chelating agents

Mice were anesthetized through inhalation of 2% isoflurane. According to the CERI Japan website, the i.p. LD50 of EDTA-Na_2 (MW = 372.24 Da) is 260 mg/kg (0.70 mmol/kg) for mice. The chelate solution of 0.70 mmol/kg (1×LD50) or 1.40 mmol/kg (2×LD50) was adjusted at 35 mM or 70 mM, respectively, and then intraperitoneally injected.

Intracolonic administration experiments were performed via laparotomy. A midline abdominal incision was made, and a catheter was inserted at the site of the proximal colon immediately distal to the cecum. We inserted a second catheter approximately 1, 5, and 8 cm (via the anus) from the first catheter in the proximal colon. Additionally, the targeted site of the colon was clamped on both the proximal and distal sides to prevent the leakage of luminal chelators. Prewarmed (50 °C) EDTA or E-PEGs (10 mM) were continuously perfused from the proximal colon to the distal colon at a flow rate of 4 mL/min to evaluate the toxicity of EDTA and E-PEGs. In the partial colon perfusion model for transplantation, 10 mM EDTA or E-PEGs (50 °C) were perfused through part (1 cm) of the proximal colon at a flow rate of 4 mL/min for 5 or 7.5 min, with mesenteric vasculature clamped during chelator perfusion[11].

Evaluation of the toxicity of EDTA and EDTA-PEGs

The acute toxicity of chelating agents after i.p. administration was determined based on clinical manifestations[41]. Under anesthesia, the mice were administered 0.70 mmol/kg or 2 × 0.70 mmol/kg of the chelating agents at 35 mM or 70 mM described above. Mice that did not show any signs of hypocalcemia in the first 15 min after administration were awakened from anesthesia. During the one-week observation period, toxicity was evaluated on a three-point scale as follows: (1) death, (2) carpopedal spasms with survival, and (3) no signs of hypocalcemia. Mice that exhibited one or more of the following lethal endpoints were considered dead and euthanized via cervical dislocation: labored breathing, decreased respiratory function, generalized convulsions, and immobility.

Blood samples for the measurement of the serum Ca levels were obtained via cardiac puncture 2 min after i.p. administration of chelating agents. In experiments involving whole or partial colonic perfusion of chelating agents, blood samples were obtained immediately after chelator perfusion. The serum Ca and albumin levels were measured using Arsenazo III and bromocresol green (BCG) assays by BML Inc. (Tokyo, Japan) and Oriental Yeast Co., Ltd. (Tokyo, Japan), respectively. Total serum Ca levels were corrected when the serum albumin level was > 4 g/dL[42]. ($n = 5$ or 6).

Evaluation of the de-epithelialized colon after treatment with the chelating agents

Colon tissue was removed from the mice immediately after perfusion with chelating agents, cut longitudinally, spread out on a rubber board with pins, and fixed overnight at 4 °C in 4% paraformaldehyde. Microscopic images of the tissue were acquired using a BZ-X800 fluorescence microscope (Keyence, Osaka, Japan) at 4× objectives to evaluate the de-epithelialized area. The de-epithelialized area, which showed higher light permeability than the surrounding regions, was analyzed using ImageJ software (NIH Image, MD, USA). Area values (mm^2) are presented for the whole-colon perfusion model. For the partial colon perfusion model, the proportion of the de-epithelialized area to the entire perfused area is presented as a percentage.

The fixed tissues were embedded in paraffin and sectioned for quantitative histological evaluation of the degree of de-epithelialization. Three different hematoxylin and eosin (H&E) sections were randomly selected from a series of sections originating from the mouse colon. All images were captured and analyzed using a Virtual Microscopy System VS 120 (Olympus Corporation, Tokyo, Japan). The degree of epithelial detachment in every part of the sections was histologically classified into three levels: Level 1, nearly intact epithelium with no denudation (no denudation); Level 2, epithelium with only the upper part denuded, leaving the bottom part of the crypts unaffected (intermediate denudation); and Level 3, epithelium with almost the entire part, including the crypt bottoms denuded (complete denudation) (Supplementary Fig. S5). The length of each level was measured, and the percentage relative to the total length of the colon in the longitudinal direction was calculated. This was performed on five mice perfused with EDTA, E-PEG4, and water, and the mean was calculated ($n = 15$).

Evaluation of blood absorption of EDTA and E-PEG4

The serum concentrations of EDTA and E-PEG4 were analyzed using LC-MS/MS by Research Center Inc. and SEKISUI MEDICAL CO., LTD. The measurement conditions described in Supplementary Table S7 were validated using mouse serum as a blank and chelating agents adjusted to concentrations of 50–50,000 ng/ml (Supplementary Fig. S9). The serum concentrations of EDTA and E-PEG4 were measured under the same conditions (Supplementary Fig. S6) ($n = 6$).

Transplantation of cultured small intestinal organoids into de-epithelialized proximal colon

The SI crypts isolated from EGFP- transgenic mice were suspended in Matrigel (BD Biosciences, NJ, USA), placed in 24-well plates, and cultured as epithelial organoids in advanced DMEM/F12 media (Thermo Fisher Scientific, MA, USA) supplemented with 500 ng/mL recombinant mouse R-spondin1 (R&D Systems, MN, USA), 20 ng/mL recombinant mouse EGF (Peprotech, Tokyo, Japan), and 100 ng/mL recombinant mouse Noggin (R&D Systems)[5,10]. The medium was changed every two days. Organoids were grown for one week, removed from Matrigel using a cell recovery solution (BD Biosciences), and suspended in a diluted Matrigel/advanced DMEM/F12 (1:2) solution. We prepared 3,000 organoids suspended in 25 µL of the solution for transplantation into each recipient mouse.

Recipient male C57BL/6J mice were treated as follows: DietGel Recovery (ClearH2O, ME, USA), a nutrient-fortified water gel, was administered for 12 h before surgery. The target segment of the proximal colon (1 cm) was de-epithelialized and perfused with 10 mM EDTA or E-PEG4 ($n=3$). DMEM containing Ca^{2+} and Mg^{2+} was subsequently added, and the vasculature of the target colon segment was clamped. The cell suspension was prepared and infused into the colonic lumen. At the end of the surgery, the recipient mice received subcutaneous injections of 2 mL of 0.9% saline solution and 25 mg/kg imipenem (Sigma-Aldrich Japan, Tokyo, Japan). They were then examined four weeks after surgery (six in total).

Stereomicroscopy, histology, and immunohistochemistry

The colon was removed from the recipient mice, cut longitudinally, and fixed overnight at 4 °C in 4% paraformaldehyde. Whole images of the targeted colonic segments and their fluorescence were acquired using a fluorescence stereomicroscope (M165FC, Leica Microsystems, Tokyo, Japan). The tissues were embedded in Tissue-Tek O.C.T. compound (Sakura Finetek Japan Co.,Ltd., Tokyo, Japan). The frozen sections were subjected to immunofluorescence staining using antibodies specific for SIase (sc-27603; Santa Cruz Biotechnology Inc. TX, USA; 1:100 dilution), LYZ (sc-27958; Santa Cruz Biotechnology Inc.; 1:300 dilution), CA2 (sc-25596; Santa Cruz Biotechnology Inc.; 1:100 dilution), OLFM4 (39141; Cell Signaling Technology. MA, USA; 1:200 dilution), Ki67 (652402; BioLegend. CA, USA; 1:200 dilution), CHGA (20085; Immunostar. WI, USA; 1:400 dilution), MUC2 (ab272692; abcam. Cambridge, UK; 1:2000 dilution), or SLC10A2 (sc-27494; Santa Cruz Biotechnology Inc.; 1:50 dilution). Nuclei were counterstained with DAPI (H-1200, Vector Laboratories, Inc., CA, USA). All images were acquired using a BZ-X800 microscope with 4× and 20× objectives. Where necessary, image processing was performed using Adobe Photoshop 23.5.5 version (Adobe, CA, USA). Sections of the $EFGP^+$ graft of EDTA- and E-PEG-treated mice and the ileum of non-operated mice (control) were subjected to immunohistochemistry for CHGA, MUC2, and LYZ for the quantitative assessment of secretory cell components. Ten crypt villus units originating from three independent recipients or controls were analyzed. The numbers of $CHGA^+$, $MUC2^+$, and LYZ^+ cells were counted and presented as the mean cell count per crypt-villus unit ($n=30$).

Quantification and statistical analysis

All data are expressed as the mean ± SEM. Biological repeats are indicated by 'n.' Statistical significance was measured using the Mann-Whitney U test for data containing two experimental groups and one-way analysis of variance with post-hoc Tukey's multiple comparison test for data containing more than two experimental groups ($^*P<0.05$, $^{**}P<0.01$, and $^{***}P<0.001$). All statistical analyses were performed using GraphPad Prism software (GraphPad Software, CA, USA).

Data availability

All data generated or analyzed during this study are included in this published article and its supplementary information files.

Received: 26 March 2025; Accepted: 16 October 2025
Published online: 20 November 2025

References

1. Tappenden, K. A. Pathophysiology of short bowel syndrome: considerations of resected and residual anatomy. *JPEN J. Parenter. Enter. Nutr.* **38**, 14S–22S. https://doi.org/10.1177/0148607113520005 (2014).
2. Pironi, L. Definitions of intestinal failure and the short bowel syndrome. *Best Pract. Res. Clin. Gastroenterol.* **30**, 173–185. https://doi.org/10.1016/j.bpg.2016.02.011 (2016).
3. Carlsson, E., Bosaeus, I. & Nordgren, S. Quality of life and concerns in patients with short bowel syndrome. *Clin. Nutr.* **22**, 445–452. https://doi.org/10.1016/s0261-5614(03)00042-6 (2003).
4. Billiauws, L. & Joly, F. Emerging treatments for short bowel syndrome in adult patients. *Expert Rev. Gastroenterol. Hepatol.* **13**, 241–246. https://doi.org/10.1080/17474124.2019.1569514 (2019).
5. Sato, T. et al. Single Lgr5 stem cells build crypt-villus structures in vitro without a mesenchymal niche. *Nature* **459**, 262–265. https://doi.org/10.1038/nature07935 (2009).
6. Kasendra, M. et al. Intestinal organoids: roadmap to the clinic. *Am. J. Physiol. Gastrointest. Liver Physiol.* **321**, G1–G10. https://doi.org/10.1152/ajpgi.00425.2020 (2021).
7. Tam, P. K. H. et al. Regenerative medicine: postnatal approaches. *Lancet Child. Adolesc. Health*. **6**, 654–666. https://doi.org/10.1016/S2352-4642(22)00193-6 (2022).
8. Nakamura, T. & Sato, T. Advancing intestinal organoid technology toward regenerative medicine. *Cell. Mol. Gastroenterol. Hepatol.* **5**, 51–60. https://doi.org/10.1016/j.jcmgh.2017.10.006 (2018).
9. Tullie, L., Jones, B. C., De Coppi, P. & Li, V. S. W. Building gut from scratch - progress and update of intestinal tissue engineering. *Nat. Rev. Gastroenterol. Hepatol.* **19**, 417–431. https://doi.org/10.1038/s41575-022-00586-x (2022).
10. Fukuda, M. et al. Small intestinal stem cell identity is maintained with functional Paneth cells in heterotopically grafted epithelium onto the colon. *Genes Dev.* **28**, 1752–1757. https://doi.org/10.1101/gad.245233.114 (2014).

11. Sugimoto, S. et al. An organoid-based organ-repurposing approach to treat short bowel syndrome. *Nature* **592**, 99–104. https://doi.org/10.1038/s41586-021-03247-2 (2021).
12. Huang, J., Xu, Z. & Ren, J. Small intestinalization of colon using ileum organoids. *Trends Cell. Biol.* **31**, 517–519. https://doi.org/10.1016/j.tcb.2021.05.002 (2021).
13. Hynes, R. O. Integrins: a family of cell surface receptors. *Cell* **48**, 549–554. https://doi.org/10.1016/0092-8674(87)90233-9 (1987).
14. Ruoslahti, E. & Pierschbacher, M. D. New perspectives in cell adhesion: RGD and integrins. *Science* **238**, 491–497. https://doi.org/10.1126/science.2821619 (1987).
15. Loftus, J. C. et al. A beta 3 integrin mutation abolishes ligand binding and alters divalent cation-dependent conformation. *Science* **249**, 915–918. https://doi.org/10.1126/science.2392682 (1990).
16. Lanigan, R. S. & Yamarik, T. A. Final report on the safety assessment of EDTA, calcium disodium EDTA, diammonium EDTA, dipotassium EDTA, disodium EDTA, TEA-EDTA, tetrasodium EDTA, tripotassium EDTA, trisodium EDTA, HEDTA, and trisodium HEDTA. *Int. J. Toxicol.* **21 Suppl 2**, 95–142. https://doi.org/10.1080/10915810290096522 (2002).
17. Desmecht, D. J., Linden, A. S., Godeau, J. M. & Lekeux, P. M. Experimental production of hypocalcemia by EDTA infusion in calves: a critical appraisal assessed from the profile of blood chemicals and enzymes. *Comp. Biochem. Physiol. Physiol.* **110**, 115–130. https://doi.org/10.1016/0300-9629(94)00156-n (1995).
18. Payne, J. M., Sansom, B. F., The relative toxicity in & rats of disodium ethylene diamine tetra-acetate, sodium oxalate and sodium citrate. *J. Physiol.* **170**, 613–620, doi:https://doi.org/10.1113/jphysiol.1964.sp007353 (1964).
19. Mehvar, R. & Shepard, T. L. Molecular-weight-dependent pharmacokinetics of fluorescein-labeled dextrans in rats. *J. Pharm. Sci.* **81**, 908–912. https://doi.org/10.1002/jps.2600810914 (1992).
20. Flessner, M. F., Dedrick, R. L. & Schultz, J. S. A distributed model of peritoneal-plasma transport: theoretical considerations. *Am. J. Physiol.* **246**, R597–607. https://doi.org/10.1152/ajpregu.1984.246.4.R597 (1984).
21. Lipinski, C. A., Lombardo, F., Dominy, B. W. & Feeney, P. J. Experimental and computational approaches to estimate solubility and permeability in drug discovery and development settings. *Adv. Drug Deliv Rev.* **46**, 3–26. https://doi.org/10.1016/s0169-409x(00)00129-0 (2001).
22. Filipski, K. J. et al. Intestinal targeting of drugs: rational design approaches and challenges. *Curr. Top. Med. Chem.* **13**, 776–802. https://doi.org/10.2174/1568026611313070002 (2013).
23. Charmot, D. Non-systemic drugs: a critical review. *Curr. Pharm. Des.* **18**, 1434–1445. https://doi.org/10.2174/138161212799504858 (2012).
24. Davis, G. R., Ana, S., Morawski, C. A., Fordtran, J. S. & S. G. & Inhibition of water and electrolyte absorption by polyethylene glycol (PEG). *Gastroenterology* **79**, 35–39 (1980).
25. Shaffer, C. B. & Critchfield, F. H. The absorption and excretion of the solid polyethylene glycols; (carbowax compounds). *J. Am. Pharm. Assoc. Am. Pharm. Assoc.* **36**, 152–157. https://doi.org/10.1002/jps.3030360507 (1947).
26. Shaffer, C. B., Nair, J. H. & Critchfield, F. H. & The absorption and excretion of a liquid polyethylene glycol. *J. Am. Pharm. Assoc. Am. Pharm. Assoc.* **39**, 340–344. https://doi.org/10.1002/jps.3030390613 (1950).
27. Hoguet, V. et al. Beyond the rule of 5: impact of pegylation with various polymer sizes on Pharmacokinetic Properties, Structure-Properties relationships of mPEGylated small agonists of TGR5 receptor. *J. Med. Chem.* **64**, 1593–1610. https://doi.org/10.1021/acs.jmedchem.0c01774 (2021).
28. Karita, S. & Kaneta, T. Chelate titrations of Ca(2+) and Mg(2+) using microfluidic paper-based analytical devices. *Anal. Chim. Acta*. **924**, 60–67. https://doi.org/10.1016/j.aca.2016.04.019 (2016).
29. Matsumoto, Y. et al. Defined serum-free culture of human infant small intestinal organoids with predetermined doses of Wnt3a and R-spondin1 from surgical specimens. *Pediatr. Surg. Int.* **37**, 1543–1554. https://doi.org/10.1007/s00383-021-04957-4 (2021).
30. Suzuki, K. et al. Single cell analysis of crohn's disease patient-derived small intestinal organoids reveals disease activity-dependent modification of stem cell properties. *J. Gastroenterol.* **53**, 1035–1047. https://doi.org/10.1007/s00535-018-1437-3 (2018).
31. Colombo, F. et al. Fluctuations of dry and total mass of cells exposed to different molecular weights of polyethylene glycol. *Adv. NanoBiomed Res.* **3** https://doi.org/10.1002/anbr.202200156 (2023).
32. Foreman, H., Vier, M. & Magee, M. The metabolism of C14-labeled Ethylenediaminetetraacetic acid in the rat. *J. Biol. Chem.* **203**, 1045–1053 (1953).
33. Hirata, H. et al. Novel diagnostic method of peritoneal injury using dual macromolecular markers. *Biol. Pharm. Bull.* **37**, 262–267. https://doi.org/10.1248/bpb.b13-00730 (2014).
34. Brady, C. E., DiPalma, J. A., Morawski, S. G., Ana, S., Fordtran, J. S. & C. A. & Urinary excretion of polyethylene glycol 3350 and sulfate after gut lavage with a polyethylene glycol electrolyte lavage solution. *Gastroenterology* **90**, 1914–1918. https://doi.org/10.1016/0016-5085(86)90261-1 (1986).
35. Sugimoto, S. et al. Reconstruction of the human colon epithelium in vivo. *Cell. Stem Cell.* **22**, 171–176e175. https://doi.org/10.1016/j.stem.2017.11.012 (2018).
36. Gonzalez, L. M., Moeser, A. J. & Blikslager, A. T. Animal models of ischemia-reperfusion-induced intestinal injury: progress and promise for translational research. *Am. J. Physiol. Gastrointest. Liver Physiol.* **308**, G63–75. https://doi.org/10.1152/ajpgi.00112.2013 (2015).
37. Li, G., Wang, S. & Fan, Z. Oxidative stress in intestinal Ischemia-Reperfusion. *Front. Med. (Lausanne).* **8**, 750731. https://doi.org/10.3389/fmed.2021.750731 (2021).
38. Ishida, T. & Kiwada, H. Anti-polyethyleneglycol antibody response to pegylated substances. *Biol. Pharm. Bull.* **36**, 889–891. https://doi.org/10.1248/bpb.b13-00107 (2013).
39. Okabe, M., Ikawa, M., Kominami, K., Nakanishi, T. & Nishimune, Y. Green mice' as a source of ubiquitous green cells. *FEBS Lett.* **407**, 313–319. https://doi.org/10.1016/s0014-5793(97)00313-x (1997).
40. Thomas, M. V. & ArsenazoIII Forms 2:1 complexes with Ca and 1:1 complexes with Mg under physiological conditions. Estimates of the apparent dissociation constants. *Biophys. J.* **25**, 541–548. https://doi.org/10.1016/S0006-3495(79)85322-9 (1979).
41. Pepe, J. et al. Diagnosis and management of hypocalcemia. *Endocrine* **69**, 485–495. https://doi.org/10.1007/s12020-020-02324-2 (2020).
42. Minisola, S., Pepe, J., Piemonte, S. & Cipriani, C. The diagnosis and management of hypercalcaemia. *BMJ* **350**, h2723. https://doi.org/10.1136/bmj.h2723 (2015).

Acknowledgements

We thank the members of the Laboratory of Morphology and Image Analysis and the Laboratory of Molecular and Biochemical Research, Research Support Center, Juntendo University Graduate School of Medicine, for their technical assistance. We also thank Jun Utsumi for the valuable advice and excellent support during this project. This study was supported by JSPS KAKENHI (19K07500, 22H03138, and 23K08038), Japan Agency for Medical Research and Development (AMED)(22hma322002h0001), and Japan Research Institute of Industrial Science. Tetsuya Nakamura belongs to the Department of Research and Development for Organoids, endowed by Eisai Co. Ltd.

Author contributions

Methodology, Investigation, and Writing – original draft, Y. Matsumoto and T.N.; Investigation, K.S. and M.T.; Investigation and Formal analyses, Y. Murakami, K.N., N.O., and S.M.; Conceptualization, G.M., H.K., N.H., K.T., and A.Y.

Declarations

Competing interests

Y. Matsumoto, TN, Y. Murakami K.N., N.O., and S.M. are inventors of a product whose patent is under application (Patent Application No: PCT/JP2021/047282). K.S., M.T., G.M., H.K., N.H., K.T., and A.Y. declare no competing interests.

Additional information

Supplementary Information The online version contains supplementary material available at https://doi.org/10.1038/s41598-025-24998-2.

Correspondence and requests for materials should be addressed to Y.M. or T.N.

Reprints and permissions information is available at www.nature.com/reprints.

Publisher's note Springer Nature remains neutral with regard to jurisdictional claims in published maps and institutional affiliations.